

Preparation and characterization of spherical $\text{Li}_{1+x}\text{V}_3\text{O}_8$ cathode material for lithium secondary batteries

Jian Gao*, Changyin Jiang, Chunrong Wan

Institute of Nuclear Energy Technology, Tsinghua University, P.O. Box 1021, Beijing 102201, PR China

Received 21 May 2003; received in revised form 14 July 2003; accepted 18 July 2003

Abstract

$\text{Li}_{1+x}\text{V}_3\text{O}_8$ is a very promising cathode material for lithium secondary batteries. A novel technique has been developed to prepare $\text{Li}_{1+x}\text{V}_3\text{O}_8$. The V_2O_5 sol is prepared via a “quencher” method by NH_4VO_3 as the raw material. Then it is mixed with LiOH solution. The spherical precursor is obtained by a spray drying method. Spherical $\text{Li}_{1+x}\text{V}_3\text{O}_8$ powders are synthesized by sintering the spherical precursor. DTA/TGA is employed to analyze the precursor. The influences of the preparing conditions including initial ratio of Li/V , sintering time and temperature on crystal structure and electrochemical performance have been investigated. As a result, the $\text{Li}_{1+x}\text{V}_3\text{O}_8$ particles obtained by sintering at 350°C for 24 h are fine, spherical, narrowly distributed, well crystallized and having excellent electrochemical properties. © 2003 Elsevier B.V. All rights reserved.

Keywords: Lithium secondary batteries; $\text{Li}_{1+x}\text{V}_3\text{O}_8$; Spray drying; Spherical

1. Introduction

Lithium vanadium oxide, $\text{Li}_{1+x}\text{V}_3\text{O}_8$ is possessed of excellent properties as the cathode materials for lithium secondary batteries. The crystal structure of $\text{Li}_{1+x}\text{V}_3\text{O}_8$ was first reported by Wadsley in 1957 [1], and also characterized by Picciotto et al. and Zhang et al. later. This vanadate has a monoclinic structure with the space group $\text{P}2_1/\text{m}$ and has a layered structure. The advantages of $\text{Li}_{1+x}\text{V}_3\text{O}_8$ as a cathode material for lithium secondary batteries are (i) the low cost, (ii) the large discharge capacity, (iii) the high discharge rate, and (iv) the long cycle life. These are caused by the following characteristics: more than three moles lithium can be accommodated per mole $\text{Li}_{1+x}\text{V}_3\text{O}_8$, high discharge rate is connected to a high diffusion coefficient of lithium, and long cycle life is due to an outstanding structural stability in lithium insertion and extraction [2–5].

As the traditional process, this kind of compound is usually prepared by high temperature synthesis [6–8]. Lithium carbonate (Li_2CO_3) and vanadium pentoxide (V_2O_5) are mixed in an agate mortar in an appropriate molar ratio. The mixture is melted on a platinum crucible in air for 24 h at 680°C . $\text{Li}_{1+x}\text{V}_3\text{O}_8$ is obtained by cooling the mixture down slowly. This method needs large thermal energy and needs

long speeding time. The electrochemical performances of the products are not satisfied.

Recently, some new synthesis methods have been used to prepare the $\text{Li}_{1+x}\text{V}_3\text{O}_8$. One of them is reported by Pistoia et al. in 1990 [9]. The $\text{Li}_{1+x}\text{V}_3\text{O}_8$ in the gel state is obtained by precipitation from an aqueous solution containing lithium hydroxide (LiOH) and vanadium pentoxide (V_2O_5). When it is dehydrated at 200°C , the oxide shows excellent electrochemical performance as an amorphous form, accommodating 4.5 moles of Li^+ ions per formula unit. Another process is reported by Kawakita et al. [10]. The $\text{Li}_{1+x}\text{V}_3\text{O}_8$ is prepared using methanol (CH_3OH) instead of water as the solvent, and lithium methoxide (LiOCH_3) is substituted for LiOH to prevent the formation of H_2O by reaction of LiOH with V_2O_5 .

In this work, the authors use a novel method to obtain V_2O_5 sol. A spray drying method is used to dry the sol. $\text{Li}_{1+x}\text{V}_3\text{O}_8$ powders are obtained after heat treatment. The structure, the morphology, and the electrochemical performance of the spherical $\text{Li}_{1+x}\text{V}_3\text{O}_8$ powders have been investigated in detail.

2. Experiment

V_2O_5 sol was prepared by a “quencher” method. NH_4VO_3 was heated at 850°C for 2 h and then quenched into deionized water. The solution was stirred at room temperature for

* Corresponding author. Tel.: +86-10-8979-6073;

fax: +86-10-6977-1464.

E-mail address: gaoj00@mails.tsinghua.edu.cn (J. Gao).

4 h and the V_2O_5 sol was obtained. Then the V_2O_5 sol and LiOH solution, in a certain molar ratio of Li:V, were mixed uniformly. The mixed sol was dehydrated via a spray drying method. The spherical $Li_{1+x}V_3O_8$ powders were synthesized by sintering the powders obtained by spray drying at 350, 450 and 550 °C, respectively, for 24 h.

Thermogravimetry and differential thermal analysis (TGA/DTA) were performed on the precursor. Powder X-ray diffraction (XRD, D/max-rB) using Cu K α radiation was used to identify the crystalline phase and crystal lattice parameters of the powders. The particle morphology, particle size and particle size distribution of the powders were observed using a scanning electron microscopy (SEM, JSM6301F).

Experimental test cells for measurements used the cathode with the composition of 80 wt.% $Li_{1+x}V_3O_8$, 10 wt.% carbon black, and 10 wt.% PTFE. The separator was a Celguard 2400 microporous polyene membrane. The electrolyte was 1 M LiPF $_6$ EC + DEC (1:1 by volume). A lithium metal anode was used in this study. The cells were assembled in a glove box filled with argon gas. The discharge–charge cycling was galvanostatically performed at a current density of 0.16 mA cm $^{-2}$ with cut-off voltages of 1.5–4.0 V (versus Li/Li $^+$) at 20 °C.

3. Results and discussion

Fig. 1 shows the TGA and DTA curves of the precursor powders obtained by spray drying at the initial ratio of Li:V = 1:2. An obvious absorbing heat peak is observed near 160 °C on DTA curve and the weight of the sample decreases up to about 310 °C by 15 wt.%. Probably, this weight loss is due to the liberation of the water molecules. A small exothermic hump is observed on DTA curve near 310 °C, at which the crystallization begins. The weight of the sample decreases gradually up to about 600 °C and no obvious peak is observed on the DTA curve. The constant weight loss between 310 and 600 °C is maybe due to the loss of lithium and oxygen in the compound. At about 600 °C, an obvious absorbing heat peak is observed on the DTA curve and the weight of the sample decreased rapidly. This weight loss is

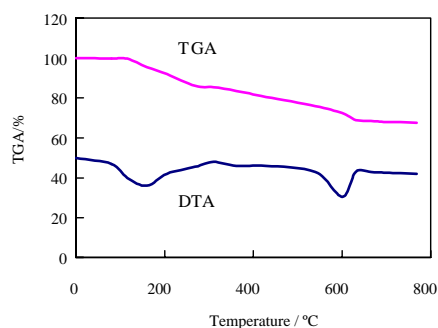


Fig. 1. DTA/TGA curves of the precursor powders by spray drying.

due to the decomposition of $Li_{1+x}V_3O_8$. Later, the weight of the sample keeps constant and no peak is observed on the DTA curve. Therefore, the range of heating temperature is selected in 310–600 °C for our experiments.

Fig. 2 shows the morphology of the precursor powders and the $Li_{1+x}V_3O_8$ powders obtained by sintering the precursor powders at different temperatures. Fig. 2a shows the particles of the precursor are spherical with the particle size of about 1–10 μ m. The surface of the every spherical particle is very smooth as shown in Fig. 2b. It is tested that the tap-density of the precursor is only 0.58 g cm $^{-3}$. In contrast to the precursor, there is obvious difference of particle morphology, particle size, particle size distribution, crystalline phase, and tap-density among the samples obtained by sintering at different temperature. Fig. 2c and d, e and f, and g and h shows the morphology of the $Li_{1+x}V_3O_8$ powders obtained by sintering at 350, 450, and 550 °C, respectively. It can be found in Fig. 2c and d that the spherical particles are shrank after sintering and the surface of the spheres is not smooth. The particle size of these samples are about 1–6 μ m and mostly are around 2 μ m. It is tested that the tap-density of this sample is as high as 1.45 g cm $^{-3}$ because of the close structure. Fig. 2e and f show the crystal grains of the $Li_{1+x}V_3O_8$ powders obtained by sintering at 450 °C are larger than the former, and the particles are not spherical because of shrinking. The crystalline grains have grown to be much larger and the spherical balls have been completely destroyed, as shown in Fig. 2g and h. The tap-density of the later two samples is only 1.33 and 1.23 g cm $^{-3}$ because of the grown crystalline grains.

In addition, the influence of initial ratio of Li/V on the SEM image and tap-density has been investigated. As a result, we found that the $Li_{1+x}V_3O_8$ products of different initial ratio of Li/V have almost the same SEM image at the same heating temperature, and the tap-density of the $Li_{1+x}V_3O_8$ product at initial ratio of Li:V = 1:2 is the highest.

The X-ray diffraction patterns of the precursor powders and the $Li_{1+x}V_3O_8$ powders obtained at different temperature are shown in Fig. 3. It can be observed that there are only some weak diffraction lines on the XRD pattern of the precursor powders. These lines were not assigned to anyone of already known vanadium oxides and lithium vanadates. Thus, the precursor sample is in an amorphous state. When heated at 350 °C, however, there are a lot of obvious diffraction lines on the XRD pattern, and all of them are attributed to $Li_{1+x}V_3O_8$. The patterns of the $Li_{1+x}V_3O_8$ powders heated at 450 and 550 °C are mostly similar to the pattern of the $Li_{1+x}V_3O_8$ powders heated at 350 °C, though the relative intensities of the former are much stronger than those of the latter and there are some new compounds appeared because of the loss of some lithium and oxygen in the former two samples. This phenomenon is explained by the deductions that the $Li_{1+x}V_3O_8$ obtained at low temperature has isotropic and strain-free crystallites and that it has the smaller grain than that obtained at high temperature. It also

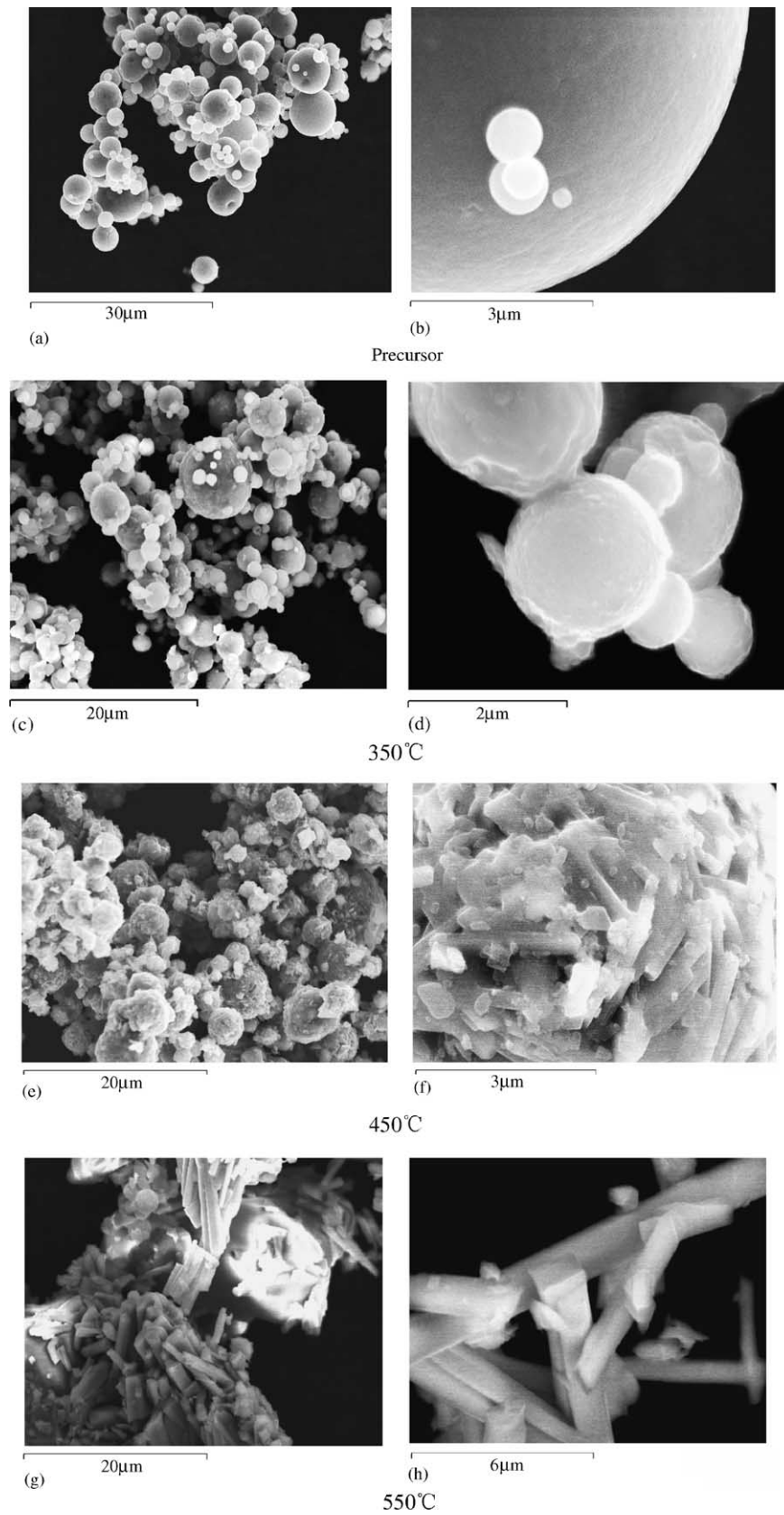


Fig. 2. SEM images of the precursor powders and the $\text{Li}_{1+x}\text{V}_3\text{O}_8$ powders at different sintering temperature.

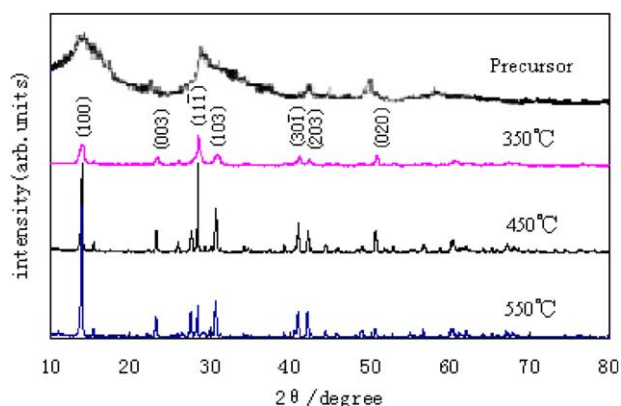


Fig. 3. X-ray diffraction pattern of the precursor and the $\text{Li}_{1+x}\text{V}_3\text{O}_8$ powders obtained at different temperature.

can be observed from the SEM images of the $\text{Li}_{1+x}\text{V}_3\text{O}_8$ powders. Different media of crystal nucleation and growth for the samples might bring about the different manner of crystal nucleation and growth [10]. The different sintering temperature results in the disparity in structure of products, and results in their different capacities. The insertion and extraction process of Li^+ ion in this cathode material is a diffusion process. With increase in sintering temperature, the intensity of (100) peak of $\text{Li}_{1+x}\text{V}_3\text{O}_8$ becomes stronger, and the crystal grains of $\text{Li}_{1+x}\text{V}_3\text{O}_8$ become larger. Thus, the diffusion path of Li^+ is longer, which is the cause of the reduction of discharge capacity of $\text{Li}_{1+x}\text{V}_3\text{O}_8$ along with increase in sintering temperature as shown afterwards.

The influence of the initial ratio of Li/V on crystal phase is obvious. If the initial ratio of Li/V is 1:3, the product includes some vanadium oxides except $\text{Li}_{1+x}\text{V}_3\text{O}_8$. But if the initial ratio of Li/V is 2:3, there are more LiVO_3 than $\text{Li}_{1+x}\text{V}_3\text{O}_8$ in the product. So we can obtain pure $\text{Li}_{1+x}\text{V}_3\text{O}_8$ only at the initial ratio of Li:V = 1:2.

The spherical $\text{Li}_{1+x}\text{V}_3\text{O}_8$ cathode materials have high specific capacity and good cycling stability compared to other vanadium system cathode materials [9]. We tested the model cells using the spherical $\text{Li}_{1+x}\text{V}_3\text{O}_8$ powders prepared in this work as the cathode material. Fig. 4 shows the

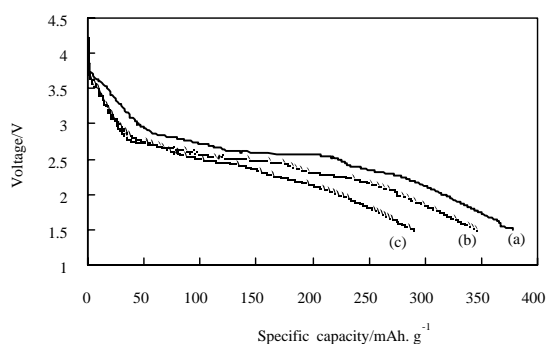


Fig. 4. First discharge curves of $\text{Li}_{1+x}\text{V}_3\text{O}_8$ prepared at different temperatures: (a) 350°C; (b) 450°C; (c) 550°C.

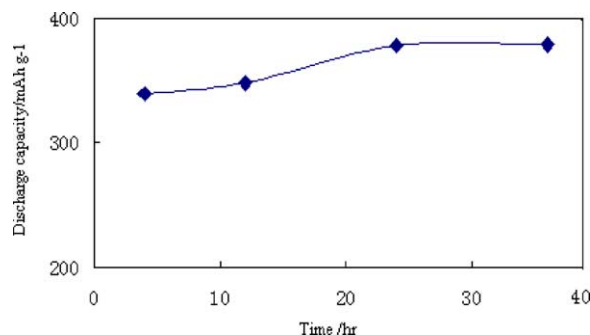


Fig. 5. The first discharge capacity of the $\text{Li}_{1+x}\text{V}_3\text{O}_8$ prepared at 350°C for different sintering time.

first discharge curves of the $\text{Li}_{1+x}\text{V}_3\text{O}_8$ obtained by heating at different temperatures. As shown in Fig. 4, the sample heated at 350°C has a first cycle discharge capacity of 378 mA h g^{-1} . However, the sample heated at 450°C has a first cycle discharge capacity of 347 mA h g^{-1} and that of the sample heated at 550°C is only 290 mA h g^{-1} . Furthermore, in the case of the sample heated at 350°C, a plateau appears clearly near 2.5 V in the discharge curve, as shown in Fig. 4a. The plateau looks much narrow in the curve of the sample heated at 450°C and in the curve of the sample heated at 550°C the plateau disappears, as shown in Fig. 4c and d. This might be explained by the ion transport rate. The smaller grain size resulted in a shorter diffusion path for Li^+ ions. The lower stacking of the layers facilitates transformation of the phase. The higher heating temperature will result in larger grains and higher stacking of the layers. In addition, the influence of sintering time on the first cycle discharge capacity has been studied. Fig. 5 shows the first cycle discharge capacity of the samples at 350°C for different sintering time. Along with the increasing of sintering time, the first discharge capacity of the product also increases. This is maybe because the structure of the sample changes more ordinal and stability during sintering. When the time arrives 24 h, the capacity does not increase any more. As a result, the best sintering time is about 24 h.

Fig. 6 shows the cycle performance of the discussed three kinds of $\text{Li}_{1+x}\text{V}_3\text{O}_8$ samples. The initial reversible specific

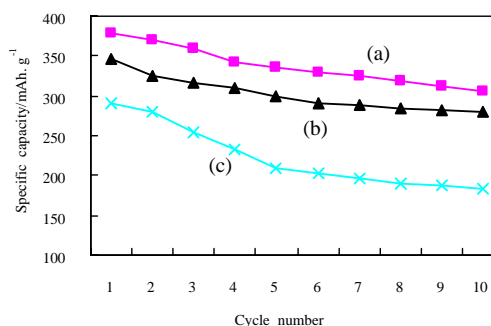


Fig. 6. Specific discharge capacity dependence on cycle number of $\text{Li}_{1+x}\text{V}_3\text{O}_8$ prepared at different temperatures: (a) 350°C; (b) 450°C; (c) 550°C.

capacity of the sample heated at 350 °C is 378 mA h g⁻¹, and after 10 cycles it is only 308 mA h g⁻¹. Unfortunately, the cycle performance of other two samples is worse than the former, because there are some new compounds appeared in the other two samples and these new compounds may lead to some negative effect on the electrochemistry performance. But it can be seen also that the cycle performance of the Li_{1+x}V₃O₈ samples is still unsatisfied. This phenomenon is connected with an outstanding structural change in the lithium insertion and extraction process. According to the report by Picciotto et al., the Li⁺ ions are reversibly inserted and extracted in a single-phase reaction when the quantity of inserted Li⁺ ions is small, whereas when the quantity of inserted Li⁺ ions is large, the reaction proceeds in the two phases system. The new phase has a defect rock-salt structure and returns to the parent structure with a slight modification during the lithium extraction process [11]. The further efforts to increase the structural stability of Li_{1+x}V₃O₈ products and the cycling performance of this material are going well.

4. Conclusion

The spherical Li_{1+x}V₃O₈ powders with high specific capacity have been synthesized via a novel technique in this work. The sample prepared at 350 °C for 24 h results the attainment of both higher discharge capacity (378 mA h g⁻¹)

and a better cycle performance. The products possess good morphology, small particle size, good particle size distribution. The excellent electrochemical performance of the spherical Li_{1+x}V₃O₈ cathode material is partly attributed to the advanced preparation. This preparation technique should be a suitable method to synthesize spherical Li_{1+x}V₃O₈ cathode material, and is significant to be further studied.

References

- [1] A.D. Wadsley, *Acta Cryst.* 10 (1957) 261.
- [2] J. Kawakita, T. Miura, T. Kishi, *Solid State Ionics* 120 (1999) 109–116.
- [3] X. Zhang, R. Frech, *Electrochim. Acta* 43 (1998) 861–868.
- [4] K. West, B. Zachau-Christiansen, S. Skaarup, et al., *J. Electrochem. Soc.* 143 (1996) 820.
- [5] G. Pistoia, M. Pasquali, Y. Geronov, et al., *J. Power Sources* 27 (1989) 35–43.
- [6] G. Pistoia, M. Pasquali, M. Tocci, et al., *J. Electrochem. Soc.* 132 (1985) 281.
- [7] J. Kawakita, Y. Katayama, T. Miura, et al., *Solid State Ionics* 107 (1998) 145–152.
- [8] G. Pistoia, M. Pasquali, Y. Geronov, et al., *J. Power Sources* 27 (1989) 35.
- [9] G. Pistoia, M. Pasquali, G. Wang, *J. Electrochem. Soc.* 137 (1990) 2365–2370.
- [10] J. Kawakita, Y. Katayama, T. Miura, et al., *Solid State Ionics* 110 (1998) 199–207.
- [11] J. Kawakita, H. Katagiri, T. Miura, et al., *J. Power Sources* 68 (1997) 680–685.